



## Improving reliability and reducing costs of cardiotoxicity assessments using laser-induced cell poration on microelectrode arrays

Giuseppina Iachetta<sup>1</sup>, Nicolò Colistra<sup>1</sup>, Giovanni Melle, Lieselot Deleye, Francesco Tantussi, Francesco De Angelis\*, Michele Dipalo\*

Istituto Italiano di Tecnologia, Via Morego 30, 16163 Genova, Italy

### ARTICLE INFO

#### Keywords:

Cardiotoxicity  
Plasmonic optoacoustic poration  
CMOS-MEA  
Intracellular recording  
hiPSC

### ABSTRACT

Drug-induced cardiotoxicity is a major barrier to drug development and a main cause of withdrawal of marketed drugs. Drugs can strongly alter the spontaneous functioning of the heart by interacting with the cardiac membrane ion channels. If these effects only surface during *in vivo* preclinical tests, clinical trials or worse after commercialization, the societal and economic burden will be significant and seriously hinder the efficient drug development process. Hence, cardiac safety pharmacology requires *in vitro* electrophysiological screening assays of all drug candidates to predict cardiotoxic effects before clinical trials. In the past 10 years, microelectrode array (MEA) technology began to be considered a valuable approach in pharmaceutical applications. However, an effective tool for high-throughput intracellular measurements, compatible with pharmaceutical standards, is not yet available. Here, we propose laser-induced optoacoustic poration combined with CMOS-MEA technology as a reliable and effective platform to detect cardiotoxicity. This approach enables the acquisition of high-quality action potential recordings from large numbers of cardiomyocytes within the same culture well, providing reliable data using single-well MEA devices and single cardiac syncytia per each drug. Thus, this technology could be applied in drug safety screening platforms reducing times and costs of cardiotoxicity assessments, while simultaneously improving the data reliability.

### 1. Introduction

Cardiotoxicity is one of the major causes associated with the drug candidate failure in clinical studies and with the withdrawal of marketed drugs (Piccini et al., 2009). In the last 60 years, 462 drugs have been withdrawn due to adverse drug effects. Among them, a significant part is related to cardiotoxicity: up to 50% in EU (McNaughton et al., 2013) and up to 22–28% in USA (Onakpoya et al., 2016). The cardiotoxicity risks could be strongly reduced if the adverse effects of therapeutic compounds were recognized in the early phases, in particular during *in vitro* measurements. Therefore, it is fundamental to improve *in vitro* methods for assessing accurately the status of all ion-channels in cardiac cells under the influence of the investigated drug.

The *in vitro* measurements of the Ether-à-go-go-Related Gene (hERG) potassium channel activity or QT prolongation have been the traditional standards for preclinical screening assay to evaluate proarrhythmic risk of new drugs (Gintant, 2011) (ICH S7B and E14 guidelines). However,

already in 2008, Lu et al. (Lu et al., 2008) questioned the predictivity accuracy of some of the ICH S7B guidelines. These considerations led to the establishment of the Comprehensive *In vitro* ProArrhythmia (CiPA) initiative (<http://cipaproject.org/>), which introduced and validated several novel tools, among which the cardiomyocytes derived from human induced pluripotent stem cells (hiPSC-CM) (Blinova et al., 2018) and the microelectrode array (MEA) as a non-invasive and label-free assay for detecting cellular arrhythmias (Blinova et al., 2018; Garg et al., 2018; Gintant et al., 2016; Sala et al., 2017; Savoji et al., 2019).

The MEA platforms have been emerging as an accessible system for recording electrical signals from cardiomyocytes with high spatial and temporal resolution (Ando et al., 2017; Clements et al., 2015; Kitaguchi et al., 2016). However, despite the extensive progresses of MEA platforms (Amin et al., 2016; Berdondini et al., 2009; Berdondini et al., 2005; Jackel et al., 2017; Jun et al., 2017; Viswam et al., 2017), current commercial MEA technologies are limited to record extracellular field potentials (FPs) instead of the action potentials (APs). Thus, they lack

\* Corresponding authors.

E-mail addresses: [francesco.deangelis@iit.it](mailto:francesco.deangelis@iit.it) (F. De Angelis), [michele.dipalo@iit.it](mailto:michele.dipalo@iit.it) (M. Dipalo).

<sup>1</sup> These authors contributed equally to this work.

the sensitivity to study the complex effects of drugs on cardiac ion channels and transmembrane ionic currents.

Recently, the novel LEAP (Local Extracellular Action Potentials) from Axion Biosystems reached the market. This method, provides detailed information about the effect of compounds on cardiac monolayers by increasing the cell-electrode coupling of cardiomyocyte syncytia on MEAs (Hayes et al., 2019). However, the low amount of recording sites provides data acquisition only from very few cells within the syncytia, rendering the drug-induced cardiotoxicity time-consuming, expensive, and not fully reliable.

Thus, there is still a lack of robust and effective tools able to provide reliable ion channel measurements with high-throughput protocols compatible with pharmaceutical standards. To this aim, we have recently introduced a novel method for obtaining high-quality AP recordings simultaneously from large cardiomyocyte networks (thousands of cells) cultured on already commercial high-density MEAs (silicon complementary metal-oxide semiconductor CMOS-MEAs) using plasmonic optoacoustic poration (Dipalo et al., 2018).

In this work, we show that the high-density recordings of cardiac APs on CMOS-MEA can drastically improve the reliability of the acquired data and thus lower the costs of cardiotoxicity assessments through the reduction of required independent experiments. We achieve the result thanks to the capability of our platform to detect high-quality APs from large numbers of hiPSC cardiomyocytes within the same culture well.

To fully support our claim and the potential of the approach, we provide a comprehensive validation of the system by using several different hiPSC-CM lines and compounds, trying thus to emulate various real-world toxicology applications. Specifically, we tested four different hiPSC-CM lines and a set of six reference compounds with inhibitory effects on cardiac ion channels and previously associated to QT prolongation and/or Torsade de Pointes (TdP) during clinical use (Colatsky et al., 2016; Kussauer et al., 2019). We show that this method allows for high-quality intracellular AP recordings of large cardiomyocyte networks, providing accurate cardiac electrophysiological parameters, such as AP shape, APD at different amplitudes, and beating rate. Furthermore, we also detect the Early After Depolarization (EADs), abnormal depolarizations during the repolarization phase of AP associated with arrhythmias (Qu et al., 2013; Weiss et al., 2010).

Based on the results, this method could be applied in screening platforms to scan efficiently and cost-effectively compounds for cardiac toxic effects, resulting in a promising tool for preclinical evaluation of new molecular entities. Since optoacoustic poration has been shown to work also on multiwell MEA plates (Melle et al., 2020), this screening methodology has the potential to be implemented in high-throughput screenings.

## 2. Material and methods

### 2.1. Human iPSC-derived cardiomyocytes

Four commercial lines of human-induced stem cell derived cardiomyocytes were used in this study: Cor.4 U and Pluricyte (Ncardia), iCell (Cellular Dynamics International), and Ventricular Cardiomyocytes (Axol Bioscience). Cor.4 U and iCell cardiomyocytes represent a mix of ventricular, atrial and nodal-like cells (Scheel et al., 2014; Yonemizu et al., 2019), whereas the other two cell lines are ventricular cardiomyocytes (Altrocchi et al., 2020; Zuppinger et al., 2017). The cells were plated directly on CMOS-MEA devices according to the specifications of the commercial supplier (including cell density, surface coating, media composition and time culture required) except for Cor.4 U. Cor.4 U cells were pre-plated in T25 culture flasks coated with fibronectin (10 µg/ml) (Sigma-Aldrich) in Dulbecco's Phosphate Buffered Saline (DPBS) and grown overnight in Cor.4 U complete medium (Ncardia) before seeding on CMOS-MEAs. This step removes dead cells prior to seeding on devices and results in better assay performance and overall data quality. The day after, pre-cultured Cor.4 U cells were

detached using Accumax solution (Sigma-Aldrich) and seeded on CMOS-MEAs.

### 2.2. Cell plating on CMOS-MEAs

The recording experiments were performed on commercial high-density CMOS-MEAs available from 3Brain AG. These CMOS-MEAs offer 4096 square recording electrodes, each  $21 \times 21 \mu\text{m}^2$  in size and placed with a  $42 \mu\text{m}$  center-to-center pitch. The devices were sterilized using 70% ethanol for 30 min and coated with the following coating solutions: geltrex ready-to-use solution for Cor.4 U cells (30 min) and fibronectin for iCell (1 h), Pluricyte and Axol Bioscience cells (3 h) at  $37^\circ\text{C}$ , 5%  $\text{CO}_2$  in a humidified incubator. Thereafter, the coating solution was aspirated and hiPSC-CMs were rapidly plated at a density of 30,000 cells per CMOS-MEA and grown with their apposite medium. Electrophysiological recordings were performed 5–8 days after plating for Cor.4 U cells, 10–14 days for iCell, 8–12 days for Pluricyte cells and after 7–10 days for Axol Bioscience Cardiomyocytes as suggested by the suppliers.

### 2.3. Laser optoacoustic poration

Laser optoacoustic poration was performed as described in Dipalo et al., 2018 (Dipalo et al., 2018) (Schematic representation in Supplementary Fig. S1). Briefly, the first harmonic ( $\lambda = 1064 \text{ nm}$ ) of a Nd:YAG (neodymium:yttrium-aluminium-garnet) solid-state laser (Plecter Duo (Coherent)) with an 8 ps pulse width and 80 MHz repetition rate was used as the radiation source for the optoacoustic poration, with an average power of approximately 1 mW after the objective. The laser was coupled to a modified upright microscope (Eclipse FN1 (Nikon)) able to accommodate the BioCAM acquisition system from 3Brain AG directly on the microscope stage. A  $60\times$  water-immersion objective (working distance 2.8 mm, numerical aperture 1.0) or a  $20\times$  air objective (working distance 20 mm, numerical aperture 0.4) was respectively used to observe the cardiomyocytes on the CMOS-MEA electrodes and to focus the NIR laser for poration. The BioCAM was mounted on top of a 2-axes motorized stage for the automatic poration of several cells by means of laser scanning.

### 2.4. Drugs and electrophysiological recordings

Nifedipine, quinidine, verapamil hydrochloride and terfenadine were purchased from Sigma-Aldrich, E-4031 and cisapride from Abcam. All compounds were dissolved in dimethyl sulfoxide (DMSO, Sigma-Aldrich) to prepare the stock solutions (10 mM), except for E-4031, which was dissolved in water. Drug dilutions were prepared in the cardiomyocyte medium suggested by the cell suppliers. The highest concentration of DMSO (0.1%) was obtained at  $10 \mu\text{M}$  drug. Before drugs treatment, 10 min of extracellular recordings were performed to characterize the cell culture. Thereafter, laser pulse trains were applied on the CMOS-MEA electrodes for porating the cardiomyocytes and recording the intracellular activity, considered as control result for later comparison. Subsequently, the compounds were added at their appropriate concentrations and, 10 min after drug exposure, poration and intracellular recordings were repeated. In details, the experimental procedure was as follow:

1. Selection of a sub-array of approximately 100 electrodes ( $10 \times 10$ ) based on cellular activity. The selection was based on cell coverage of the array and on the quality of the field potentials. In fact, high amplitude field potentials indicate tight cell adhesion on the electrode, which in turn promotes high-quality intracellular recording after poration.
2. Focusing the laser on the electrode in the center of the sub-array.
3. Laser poration of the cells on the whole sub-array by using a laser scanner system that applies 1 laser pulse on each electrode.

4. Acquisition of action potentials for few minutes.
5. Administration of the drug at 1<sup>st</sup> concentration.
6. 10 min waiting time.
7. Repetition of steps from 1 to 4.
8. Administration of the drug at 2<sup>nd</sup> concentration.
9. 10 min waiting time.
10. Repetition of steps from 1 to 4.

The concentrations of each tested drug were derived from published literature (Braam et al., 2010; Harris et al., 2013; Kuusela et al., 2016). Drug effects were evaluated by increasing drug concentration in the same well. All recordings were performed at 37 °C outside the incubator. The cell medium from each sample was changed approximately 2 h before the experiments.

## 2.5. Data and statistical analysis

At first, the CMOS-MEA data were acquired by means of the 3Brain® software “Brainwave X”. Subsequently, a custom-made algorithm was specifically developed in MATLAB (The Mathworks, Natick, MA, USA) to perform further data analysis. This algorithm allows for a proper and accurate characterization of the intracellular action potentials waveforms recorded from hiPSC-derived cardiomyocytes. AP detection was performed by carefully setting the amplitude threshold and refractory period both in control conditions and after drug administration. Moreover, in order to discriminate the intracellular APs from the extracellular ones, a specific threshold (*i.e.* 10 ms) applied to the action potential duration (APD) at 10% repolarization was adopted. In such a way, the extracellular spikes, which have a typical duration of approximately 5 ms, are rejected, whereas the intracellular APs are passed on for further analysis. To analyse and quantify the electrophysiological activity of the cardiac cells, several action potential parameters were extracted from the analysis. In particular, we evaluated the beating rate, the intracellular action potential mean waveforms of the active channels and the intracellular APs duration at different amplitude values with respect to the maximum amplitudes (30%, 50% and 90%). Data were expressed as mean ± standard error. Statistical analysis was performed to determine significant differences between all sample pairs by using MATLAB. Since data do not follow a normal distribution (evaluated by the Kolmogorov-Smirnov normality test), a non-parametric Mann-Whitney *U* test was used. In all cases, significance was defined as  $p \leq 0.05$ .

## 2.6. Live/Dead assay and immunofluorescence

Cell viability after laser optoacoustic poration was tested using Live/Dead assay (ThermoFisher L3224). Calcein acetoxymethyl (Calcein AM) and ethidium homodimer dyes were added to the cells according to the supplier’s instruction. The cells were imaged with Nikon Eclipse FN1 by using filters for FITC channel (ex/em 494/517 nm) and TRITC channel (ex/em 528/617 nm) with a 20× air objective. Live cells are stained with green fluorescence, whereas dead cells with red fluorescence. Furthermore, immunofluorescence for cardiac troponin-T (TNNT2/cTnT), a marker for cardiomyocytes, was performed on hiPSC-CMs after laser optoacoustic poration by using Human Cardiomyocyte Immunocytochemistry Kit (Life Technologies A25973). Briefly, after fixation with 4% (*w/v*) formaldehyde in DPBS for 15 min the cells were incubated with the permeabilization solution (1% Saponin in DPBS) for 15 min and then with a blocking solution (3% bovine serum albumin) for 30 min. Thereafter, the cells were incubated with primary antibody (mouse anti-TNNT2 A25969) diluted 1:1000 in the blocking solution for 3 h at room temperature followed by washing 3 times with wash buffer and incubation for 1 h at room temperature with secondary antibody (Alexa Fluor 488 donkey anti-mouse) diluted 1:250 in blocking solution. Finally, cells were counterstained with DAPI and imaged on Nikon Eclipse FN1 microscope with an air 20× objective or a water immersion 60× objective, using filters for Alexa 488 channel (Ex/Em 495/519 nm)

and DAPI channel (Ex/Em 358/461 nm).

## 3. Results

### 3.1. Field potential and action potential recordings

Field potential and action potential recordings on hiPSC-CMs were performed using the experimental set-up shown in Fig. 1A, which consisted mainly in a CMOS-MEA acquisition system, a laser source and an optical microscope. The recordings were obtained by applying the optoacoustic poration protocol on several electrodes of the CMOS-MEAs using an automatic system for laser scanning over the cell culture. In Fig. 1B, we report the main elements of our experimental protocol. Before cell poration, we record field potentials from the majority of the electrodes of the CMOS-MEA. The field potentials are generally bi-phasic with a short duration below 20 ms, as exemplified in the top-left panel of Fig. 1B. Supplementary Video S1 shows an exemplary spontaneous propagation wave in a hiPSC-CM syncytium on the 4096 electrodes of a CMOS-MEA. The pixel colors indicate potential variations over time.

Then, we select a sub-population of 50–100 cells in the cardiac culture and we apply optoacoustic poration, recording thus action potentials from this sub-population as control data (square “1” in the false-color map representing the APD50 values on the CMOS-MEA electrode array). Subsequently, we administer the drug at a certain concentration and perform poration and recording on a second sub-population of the same culture (square “2” in the false-color map). This step is repeated for as many concentrations of drugs are tested. The details of the complete experimental procedure are reported in the Materials and Methods section. On the right of Fig. 1B, we report exemplary action potential shapes for the three regions on the false-color map. To highlight the benefits of recording intracellular action potentials, in Supplementary Fig. S2 we report close views of exemplary extracellular field potentials and action potentials before and after administration of drugs. We can observe that the drug effects on the field potentials are only visible by significantly enlarging the amplitude scale, whereas they are easily quantifiable on the intracellular action potentials. For comprehensiveness, we also report in Supplementary Fig. S8 a comparison between the distributions of APD50 (measured in the intracellular action potentials) and QT intervals (measured by the extracellular field potentials) from iCell cardiomyocytes.

The plasmonic optoacoustic poration of the cellular membrane is a very localized a non-invasive process that does not perturb the cells and their electrophysiological activity. This stems from (I) the limited area of effect, confined to the focused laser spot of about 2 μm in diameter, (II) the ultra-fast pulsed laser that concentrates the optical energy in very short packages, and (III) the plasmonic response of the electrode that enhances the laser effect and allows for reducing its intensity (Dipalo et al., 2018). All together, these properties provide cell poration in very mild conditions. As previously reported, AP recordings with plasmonic optoacoustic poration may last from few minutes up to 30 min, with the signals recovering field potential features after cellular membrane reformation. Fig. 1C reports a bright field image of hiPSC-CMs on CMOS-MEA electrodes after cell optoporation (left), the same cells stained with cardiac Troponin T (middle), and a representative live/dead assay of hiPSC-CMs after optoporation. The viability assay displays a uniform syncytium of healthy cardiomyocytes, whereas immunofluorescence highlights normal structures of cardiac Troponin T, an important indicator of healthy cardiomyocyte cultures. Therefore, the intracellular recording procedure has no significant effects on the cell health. In Supplementary Figs. S3–S5, we report further images of viability assays and immunofluorescence of hiPSC-CMs (iCell) on CMOS-MEA after application of plasmonic optoporation.

The action potentials presented throughout the manuscript show maximum amplitudes of 4 mV, as this is the limit of the amplification chain of the CMOS-MEA devices. The future employment of other MEA platforms with higher amplitude limits will enable the recording of actin

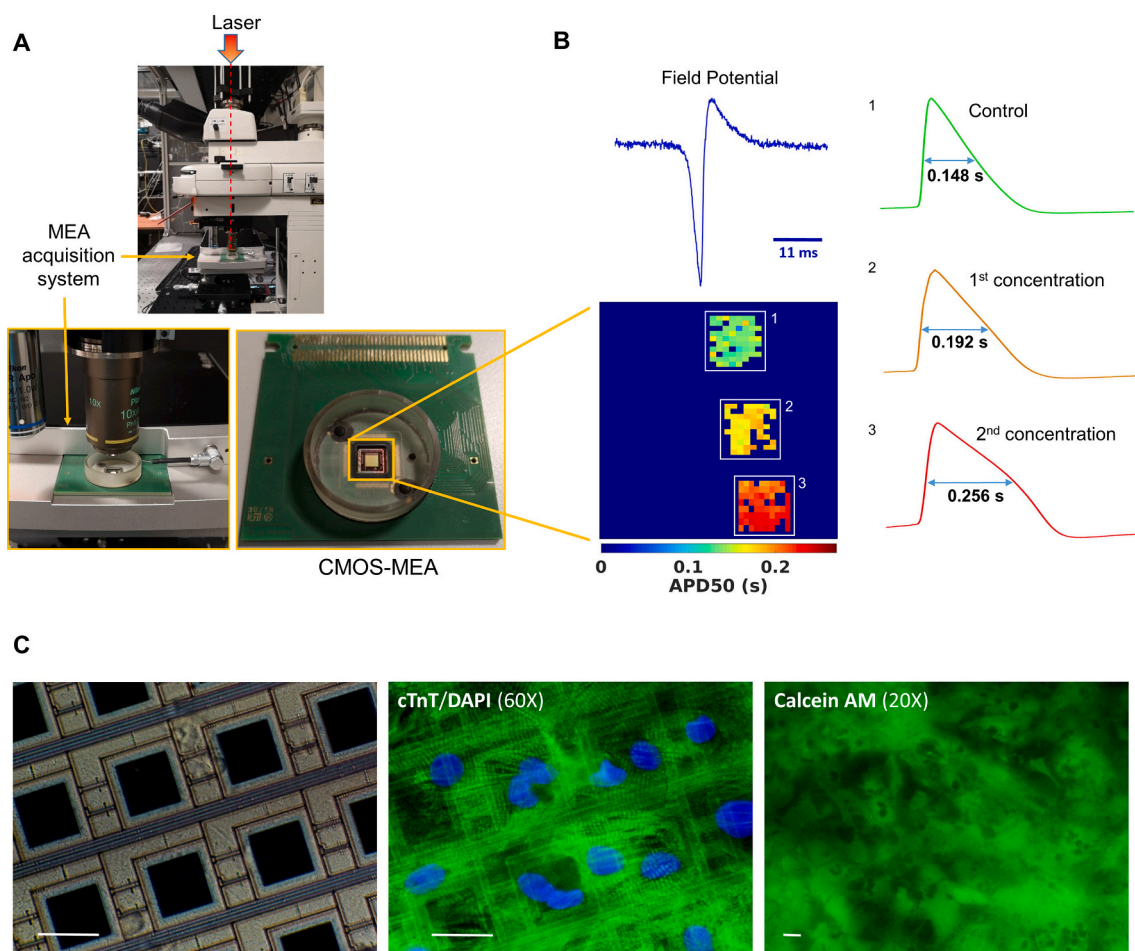


**Fig. 1.** (A) Photographs showing the experimental set-up used for laser optoacoustic poration and intracellular recording on large cell networks. (B) Exemplary CMOS-MEA false-color map (bottom) of the APD50 values of intracellular action potentials and time traces (right) from the map showing the averaged action potential shapes of Pluricytes for three different regions (1, 2 and 3) at different concentrations of quinidine (control, concentration 1 and concentration 2). On the top-left panel, an exemplary field potential before optoacoustic poration is shown. (C) Representative images of hiPSC-CMs on CMOS-MEA in bright field, Cardiac Troponin T (cTnT) and DAPI, and Calcein AM. Scale bar 20  $\mu\text{m}$ .

potentials with larger amplitudes. In fact, in a previous publication, we have shown that intracellular signals with higher amplitude can be recorded using optoporation (Melle et al., 2020).

### 3.2. Effects of reference compounds on cardiomyocytes

In order to evaluate the efficacy and the versatility of our method in cardiac safety drug screenings, we tested it using six drugs with ion channel blocking properties and previously associated with QT prolongation and/or TdP during clinical use in humans on different commercial hiPSC cardiomyocytes. The tested drugs had either selective ion channel blocker or mixed ion channel blocker properties. On one of the cell lines (iCell), we tested all drugs in order to provide a comprehensive picture of the effects on a specific cellular model (Supplementary Fig. S6). Two of the drugs (nifedipine and quinidine) were also used to compare and discern differences in AP morphology across hiPSC-CM lines. Furthermore, two drugs withdrawn from market, associated to intermediate TdP risk, were tested on multiple cell lines. Finally, aspirin, a non-steroidal anti-inflammatory drug known to have no effect on cardiomyocyte activity (Asakura et al., 2015), was chosen as negative control (Supplementary Fig. S7). All the tested compounds have well-known acute (short-term) effects that occur just few minutes after their administration to cardiac cultures (Asahi et al., 2018; Dempsey et al., 2016; Harris et al., 2013; Kitaguchi et al., 2016; Meyer et al., 2004; Nozaki et al., 2017; Pfeiffer-Kaushik et al., 2018). Hence, we recorded

the compound's effects always 10 min after administration.

The tested drugs and hiPSC-CM lines are summarized in Table 1. To characterize the electrical activity of the cardiac cells before and after drug administration, the following parameters were evaluated: duration of action potential (APD) and its shape, time needed to reach 30%, 50% and 90% repolarization and beating rate.

To improve the reliability of the screenings, we performed all measurements maintaining comparable conditions. The culture temperature was kept at 37 °C during recordings, whereas medium change was always performed 2 h before the measurements. Moreover, cells were taken out from the incubator only right before recordings, keeping thus a constant "out-of-incubator" period across the cultures.

#### 3.2.1. E-4031

E-4031, a specific hERG channel blocker, induces AP lengthening

**Table 1**  
List of the tested drugs and commercial hiPSC-CM lines.

| Compound type                 | Drug        | Tested Cell lines |
|-------------------------------|-------------|-------------------|
| Selective ion channel blocker | E-4031      | Pluricyte         |
|                               | Nifedipine  | Cor.4 U iCell     |
| Mixed ion channel blocker     | Quinidine   | Pluricyte iCell   |
|                               | Verapamil   | Cor.4 U           |
| Withdrawn from market         | Cisapride   | Pluricyte         |
|                               | Terfenadine | Axol Bioscience   |

and EADs often associated with cardiac arrhythmias (Kuusela et al., 2016; Mohammad et al., 1997). We observed a significant prolongation of the APD compared to the control. Moreover, EADs occurred for both E-4031 tested concentrations (Fig. 2A). Furthermore, our data show that E-4031 leads to the reduction of the beating rate (minor at 1  $\mu$ M and substantial at 2  $\mu$ M concentration) (Fig. 2B). The analysis of the intracellular APs shows that the APD lengthening occurs at 30%, 50% and 90% repolarization for both concentrations (Fig. 2C). Thanks to the uninterrupted recording during cell poration and drug administration, we are also able to observe the temporal dynamic evolution of E-4031 effects on hiPSC-CMs. This is demonstrated in Fig. 2D, where we report APs immediately after administration of 2  $\mu$ M E-4031. The EADs appear gradually in the APs, in correspondence to the significant prolongation of the repolarization phase.

### 3.2.2. Nifedipine

Nifedipine, a common L-type calcium channel blocker, is known to decrease the AP duration and increase the beating rate in cardiomyocytes (Guo et al., 2011; Harris et al., 2013; Huo et al., 2017). Our results show that nifedipine clearly induces a dose-dependent APD shortening compared to the control in both Cor.4 U and iCell cardiomyocytes (Fig. 3A, D), according to the previously reported data. The effect of nifedipine is observed in both cell lines, which can be distinguished by the different AP shape corresponding to the different cellular model. Nifedipine also significantly increases the beating rate in a concentration-dependent manner in both Cor.4 U and iCell cardiomyocytes (Fig. 3B, E). We quantify the concentration-dependent effect of nifedipine by plotting the APD at 30%, 50% and 90% repolarization levels (Fig. 3C, F).

### 3.2.3. Quinidine

We tested the effect of quinidine, a well-characterized class 1 antiarrhythmic compound strongly associated with TdP in patients.

Quinidine acts as hERG channel blocker with mild to weak sodium and calcium channel blocking properties (Bauman et al., 1984; Kramer et al., 2013). Quinidine is known to prolong the AP duration in different cardiomyocytes (Kuusela et al., 2016; Mehta et al., 2014; Navarrete et al., 2013). In our measurements, we observed that quinidine causes a dose-dependent prolongation of APD compared to the control in Pluricyte and iCell cardiomyocytes (Fig. 4A and D). In addition, in iCell cardiomyocytes, we detected EADs at 2  $\mu$ M and 10  $\mu$ M drug concentration (Fig. 4D). Quinidine induces arrhythmia in Pluricyte and iCell cardiomyocytes at all tested concentrations (Fig. 4B and E). In Fig. 4C and F, we report the quantification of the effects on the APD at 30%, 50% and 90% repolarization levels for all concentrations (Fig. 4C and F).

### 3.2.4. Verapamil

Verapamil is a well-characterized class IV antiarrhythmic drug used to treat cardiac arrhythmias. This drug has multichannel properties, blocking both the hERG potassium channel and the L-type calcium channel (Aiba et al., 2005). Verapamil significantly reduces the AP (Blinova et al., 2017; Mehta et al., 2014) and increases the spontaneous beating rate of hiPSC-CM in a dose-dependent manner (Harris et al., 2013). Consistently with published literature, we observed that verapamil significantly shortened the APD compared to the control (Fig. 5A) and produced a concentration-dependent increase in the beating rate of Cor.4 U cardiomyocytes (Fig. 5B). The data analysis shows that verapamil induces a reduction of APD at 30%, 50% and 90% repolarization at all tested concentrations (Fig. 5C).

### 3.2.5. Cisapride

Cisapride is a serotonin 5-HT<sub>4</sub> receptor agonist known to block the hERG potassium channel and with weak to mild sodium and calcium channel blocking properties (Kramer et al., 2013; Mohammad et al., 1997; Nozaki et al., 2017). This drug has been used to treat several gastrointestinal disorders, such as gastro-esophageal reflux, and has

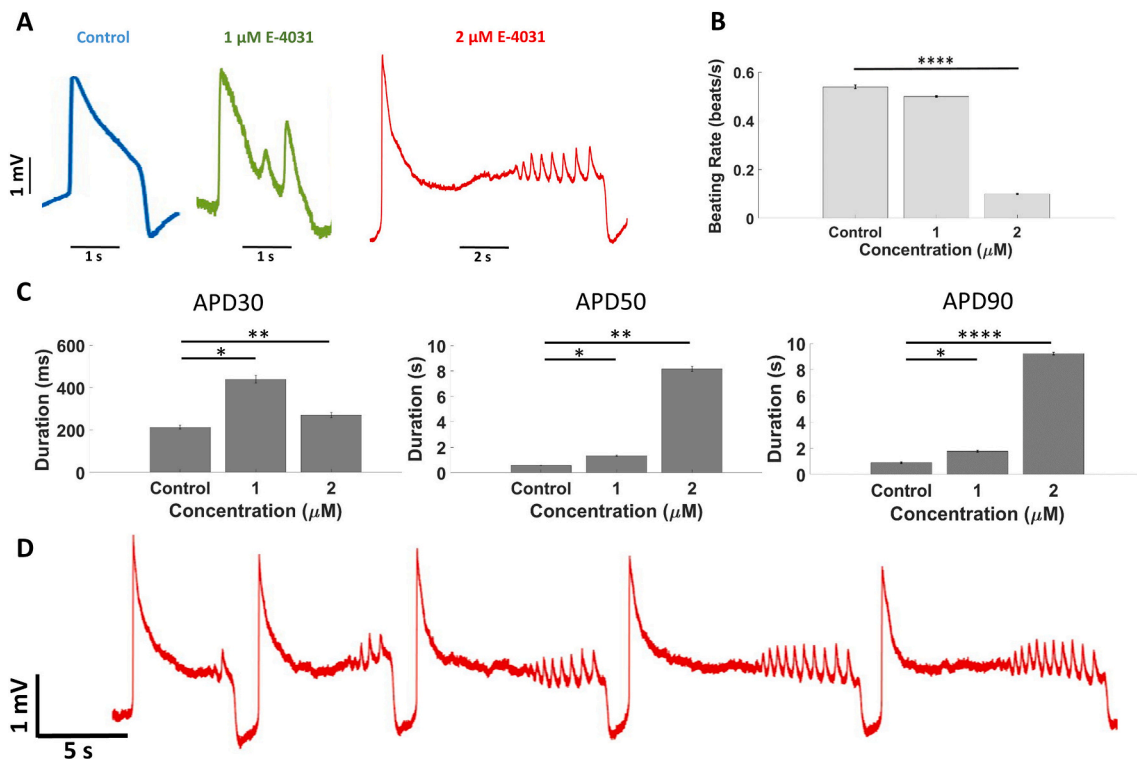


**Fig. 2.** Effects of E-4031 on intracellular action potentials recorded from Pluricyte. (A) Action potential waveforms in control conditions and at tested concentrations of E-4031, which show clear early afterdepolarizations (EADs). (B) Beating rate before (Control) and after E-4031 administration. (C) APD at different amplitudes (APD30, 50, 90). (D) Temporal dynamic evolution of APs after administration of 2  $\mu$ M E-4031. Data are represented as mean  $\pm$  SEM.  $N = 70$  (Control and 1  $\mu$ M),  $N = 95$  (2  $\mu$ M).  $P$ -values are calculated using Mann-Whitney  $U$  test,  $*0.01 < P < 0.05$ ,  $**0.001 < P < 0.01$ ,  $***0.0001 < P < 0.001$ ,  $****P < 0.0001$ .

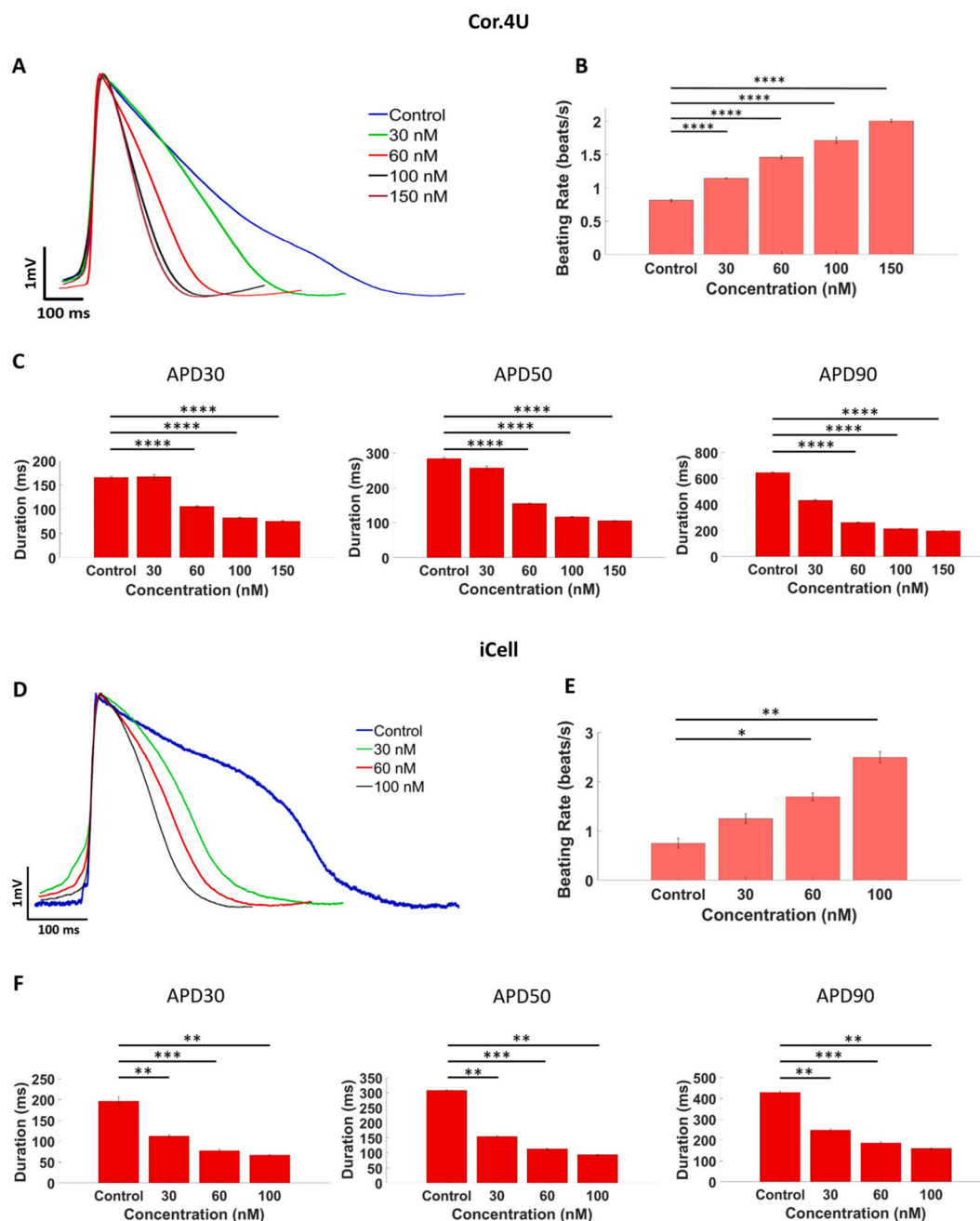


**Fig. 3.** Concentration-dependent effects of nifedipine on intracellular action potentials recorded from Cor.4 U and iCell cardiomyocytes. (A, B and C) Cor.4 U action potential waveforms, beating rate and APD at different amplitudes (APD30, 50, 90). (D, E and F) iCell action potential waveforms, beating rate and APD at different amplitudes (APD30, 50, 90). Data are represented as mean  $\pm$  SEM.  $N = 80$  (Control),  $N = 65$  (30 nM),  $N = 92$  (60 nM),  $N = 115$  (100 nM),  $N = 121$  (150 nM) for Cor.4 U.  $N = 60$  (Control),  $N = 65$  (30 nM),  $N = 78$  (60 nM),  $N = 105$  (100 nM) for iCell.  $P$ -values are calculated using Mann-Whitney  $U$  test,  $*0.01 < P < 0.05$ ,  $**0.001 < P < 0.01$ ,  $***0.0001 < P < 0.001$ ,  $****P < 0.0001$ .

been withdrawn from the US market in 2000 due to its serious cardiac side-effects (Food and Administration, 2000; Wysowski and Bacsanyi, 1996). Cisapride induces QT prolongation and/or TdP in patients (Darpö, 2001) and concentration-dependent AP prolongation in hiPSC-CM (Kuusela et al., 2016; Mehta et al., 2013). Using our approach, we could replicate these observations. Cisapride leads to a prolongation of the APD in cardiomyocytes and a reduction of the beating rate in a concentration-dependent manner (Fig. 6A and B). Furthermore, cisapride prolongs the action potential duration at 30%, 50% and 90% repolarization at all tested concentrations (Fig. 6C).

### 3.2.6. Terfenadine

Terfenadine, a non-sedating antihistamine, was withdrawn from the US market in late 1997 due to the risk of cardiac arrhythmia caused by QT prolongation (Redfern et al., 2002; Food and Administration, 1997). This drug acts blocking multiple cardiac ion channels. In particular it acts on the hERG, sodium and calcium channels (Lu et al., 2012; Ming and Nordin, 1995). In hiPSC-CMs, terfenadine induces AP lengthening at low concentration and AP shortening at higher concentration (Asahi et al., 2018; Braam et al., 2010; Harris et al., 2013; Liu and Melchert, 1997). On ventricular cardiomyocytes, our results indicate that terfenadine significantly prolonged the APD at 10 nM and 100 nM, whereas it shortened the APD at 1  $\mu$ M (Fig. 7A), as previously reported by other

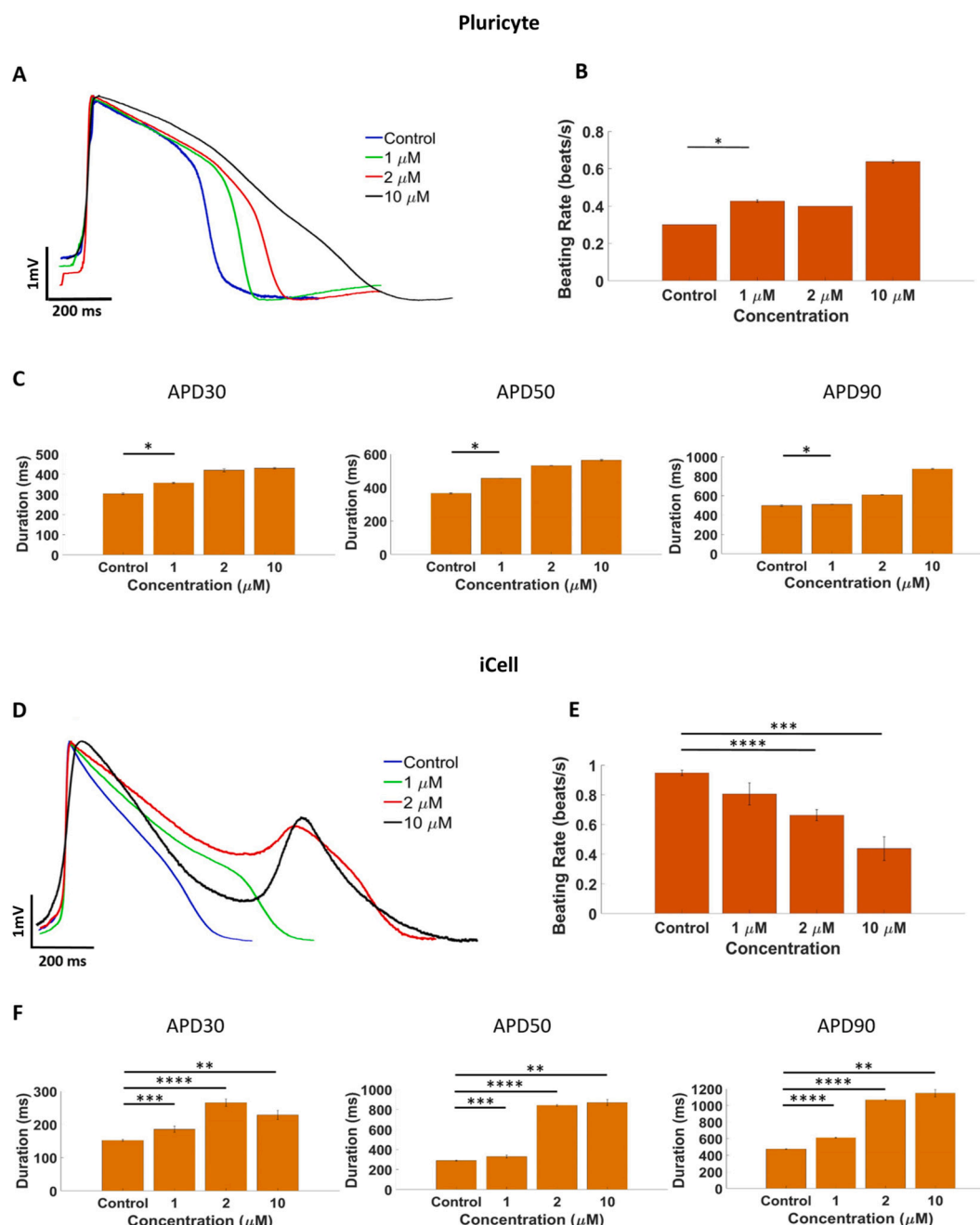


**Fig. 4.** Concentration-dependent effects of quinidine on intracellular action potentials recorded from Pluricyte and iCell cardiomyocytes. (A, B and C) Pluricyte action potential waveforms, beating rate and APD at different amplitude (APD30, 50, 90). (D, E and F) iCell action potential waveforms with early after-depolarizations (EADs), beating rate and APD at different amplitude (APD30, 50, 90). Data are represented as mean  $\pm$  SEM.  $N = 40$  (Control),  $N = 50$  (1  $\mu\text{M}$ ),  $N = 50$  (2  $\mu\text{M}$ ),  $N = 6$  (10  $\mu\text{M}$ ) for Pluricyte.  $N = 64$  (Control),  $N = 48$  (1  $\mu\text{M}$ ),  $N = 46$  (2  $\mu\text{M}$ ),  $N = 35$  (10  $\mu\text{M}$ ) for iCell. P-values are calculated using Mann-Whitney U test,  $*0.01 < P < 0.05$ ,  $**0.001 < P < 0.01$ ,  $***0.0001 < P < 0.001$ ,  $****P < 0.0001$ .

groups (Asahi et al., 2018; Braam et al., 2010; Harris et al., 2013). This effect was observed at all amplitude levels (Fig. 7C). Terfenadine also leads to a reduction in beating rate at 10 and 100 nM concentrations. Differently, we observed an increase of beating rate at 1  $\mu\text{M}$  in comparison to the previous tested concentrations (Fig. 7B).

#### 4. Discussion

With our experiments, we demonstrate that the use of plasmonic optoacoustic poration combined with CMOS-MEA technology can drastically improve the reliability of drug screenings, allowing for the reduction of the cell cultures required to reach exploitable results in

cardiac safety screenings. We validate our findings by using a comprehensive set of reference drugs with ion channel inhibitory effects and associated with QT prolongation and/or Torsade de Pointes (TdP) during clinical trials. Our measurements demonstrate that the effects of these drugs can be accurately assessed *in vitro* using laser cell poration on large two-dimensional syncytia of hiPSC cardiomyocytes, exposing the alterations in the action potential shape and in the beating rate. After nifedipine and verapamil administration, we observed concentration-dependent responses of both APD and beating rate, with a progressive APD shortening, a change of its shape and an increase of spontaneous beating rate. For E-4031 and quinidine, we found an APD prolongation and a beating rate reduction in a concentration-dependent manner,

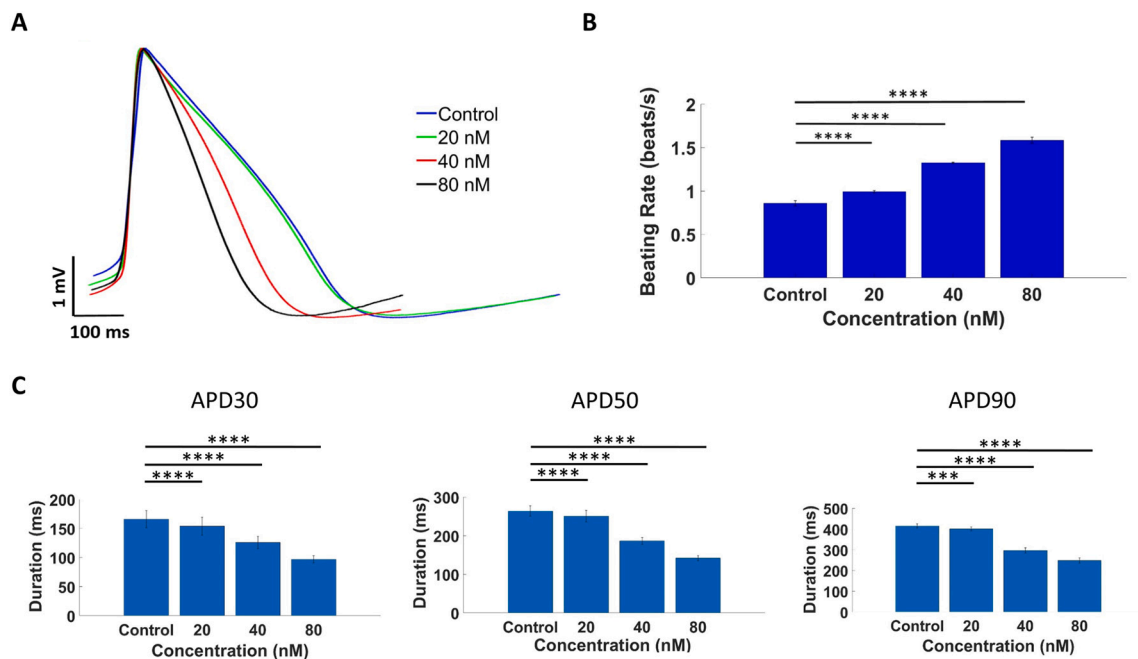


**Fig. 5.** Concentration-dependent effects of verapamil on intracellular action potentials recorded from Cor.4 U cardiomyocytes. **(A)** Action potential waveforms recorded in control conditions and at increasing amounts of verapamil. **(B)** Beating rate before and after verapamil administration. **(C)** APD at different amplitudes (APD30, 50, 90). Data are represented as mean  $\pm$  SEM.  $N = 51$  (Control),  $N = 55$  (20 nM),  $N = 67$  (40 nM),  $N = 40$  (80 nM). P-values are calculated using Mann-Whitney U test,  $*0.01 < P < 0.05$ ,  $**0.001 < P < 0.01$ ,  $***0.0001 < P < 0.001$ ,  $****P < 0.0001$ .

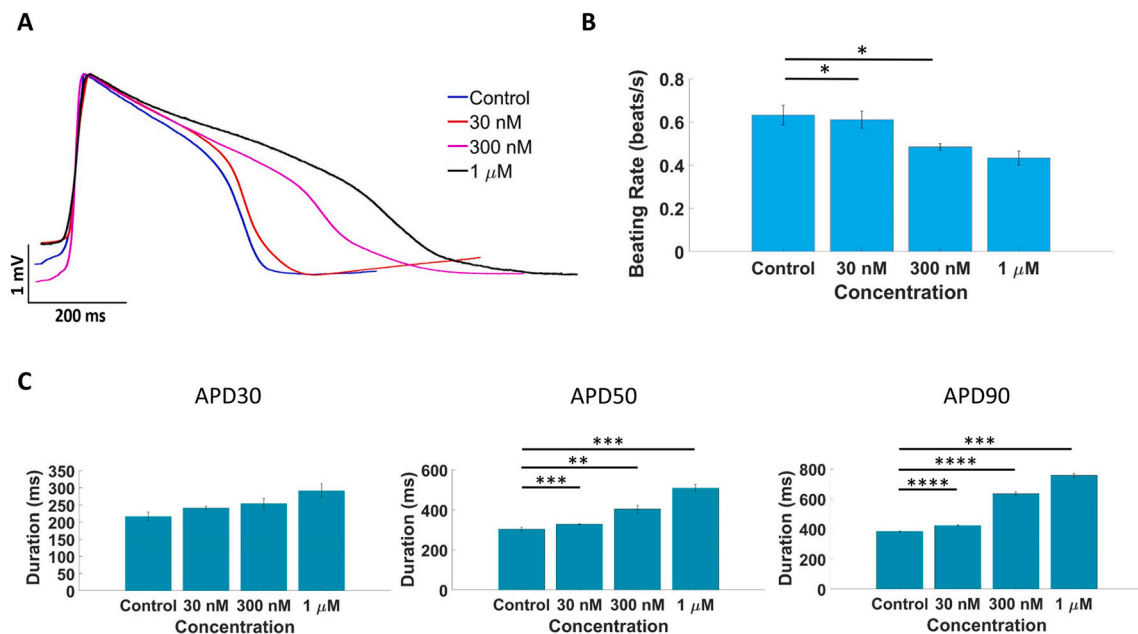


**Fig. 6.** Concentration-dependent effects of cisapride on intracellular action potentials recorded from Pluricyte. **(A)** Action potential waveforms were recorded in control conditions and at increasing amounts of cisapride. **(B)** Beating rate before (Control) and after cisapride administration. **(C)** APD at different amplitudes (APD30, 50, 90). Data are represented as mean  $\pm$  SEM.  $N = 70$  (Control),  $N = 75$  (30 nM),  $N = 95$  (300 nM),  $N = 50$  (1  $\mu$ M). P-values are calculated using Mann-Whitney U test,  $*0.01 < P < 0.05$ ,  $**0.001 < P < 0.01$ ,  $***0.0001 < P < 0.001$ ,  $****P < 0.0001$ .

detecting also the expected EADs occurrence after drug administration. Finally, we observed the APD prolongation and the beating rate reduction at all tested concentrations for cisapride and the APD prolongation at low concentrations and APD shortening at higher concentration for terfenadine, associated with alterations in the beating rate. We also analyzed the APD at different amplitudes (30%, 50% and 90% repolarization) obtaining the detailed profile of drug effects. In addition, we

report an example of the high potential of our approach for observing the temporal dynamic evolution of drug effects on hiPSC-CMs. Specifically, we report the gradual appearance of EADs exploiting the uninterrupted recording during cell poration and E-4031 administration. Finally, we acquired data from cultures of different hiPSC cardiac models provided commercially by various suppliers. The high quality of the recorded signals allowed us to observe the expected different AP

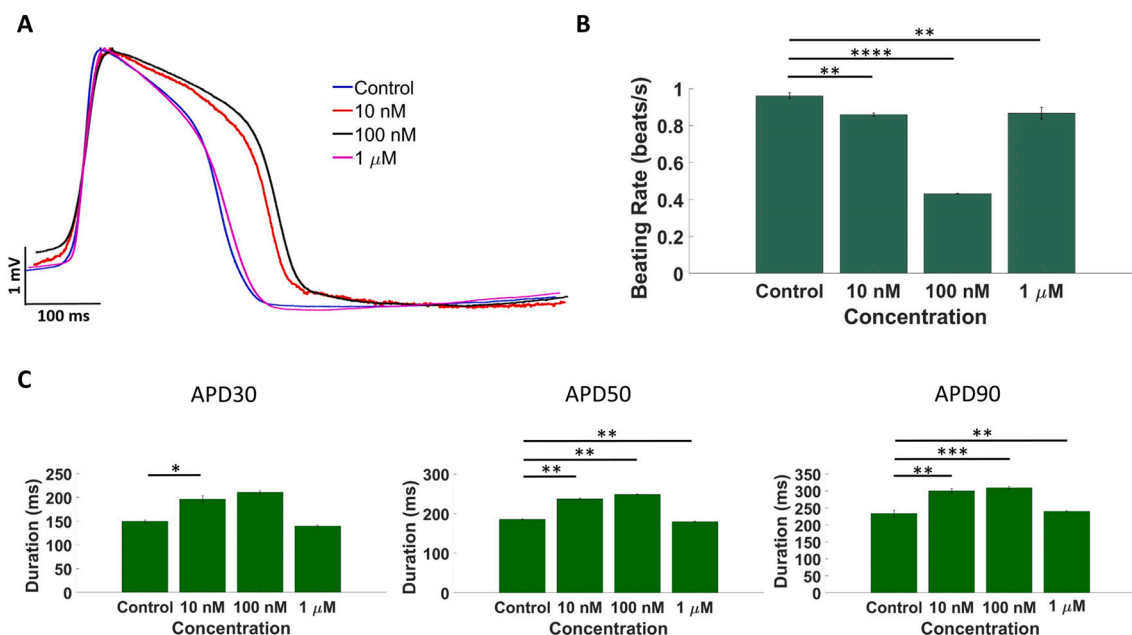


**Fig. 7.** Concentration-dependent effects of terfenadine on intracellular action potentials recorded from Axol Bioscience cardiomyocytes. **(A)** Action potential waveforms were recorded in control conditions (Control) and at increasing amounts of terfenadine. **(B)** Beating rate before and after terfenadine administration. **(C)** APD at different amplitudes (APD30, 50, 90). Data are represented as mean  $\pm$  SEM.  $N = 70$  (Control),  $N = 50$  (10 nM),  $N = 86$  (100 nM),  $N = 50$  (1  $\mu$ M). P-values are calculated using Mann-Whitney U test, \* $0.01 < P < 0.05$ , \*\* $0.001 < P < 0.01$ , \*\*\* $0.0001 < P < 0.001$ , \*\*\*\* $P < 0.0001$ .

shapes of the various cell lines.

Such a large amount of reliable data from six compounds and four hiPSC-CM lines has been obtained using only 12 cell-culture wells in total, which is an exceedingly low number of experiments. Thus, the presented approach provides accurate parameters based on intracellular AP recordings and at the same time reduces the number of required experiments. This may result in higher predictivity, lower culture variability and reduced number of experiments.

The CMOS-MEA biosensors employed in this work did not offer stimulation or pacing capabilities. Therefore, our measurements were limited to spontaneously beating cultures. However, in perspective, we do not forecast technical limitations in applying plasmonic optoporation for obtaining intracellular recordings on paced cultures, exploiting more recent high-density MEAs that provide stimulation functionalities (“3Brain HD-MEAs,” 2021, “Maxwell Biosystems MEAs,” 2021). In fact, these newer devices share similar electrode materials and morphologies to those employed in our work. Hence, plasmonic optoporation will be most likely feasible on them.

## 5. Conclusions

In summary, the acquired data highlight all the expected effects of the evaluated drugs, confirming the validity and the high potential of *in vitro* MEA recordings enhanced by laser cell poration and high electrode density. In particular, the parallelization of the procedure over several cells within the same culture provides reliable data even using single-well MEA devices and single syncytia per each drug. This could represent an advantage for reducing the amount of experiments required to obtain consistent results. Even using more cultures for avoiding incremental concentrations of drugs in the same wells, the results of this work on 6 drugs, several concentrations, and 4 cell lines, could have been obtained by using a total number of 28 wells. This amount of wells is still extraordinary small if we consider that multiwell MEA plates with high-density CMOS-MEAs have begun to appear recently on the market (“3Brain MultiplEx,” 2021; “Maxwell Biosystems MaxTwo,” 2021). Thus, laser cell poration and high-resolution multiwell MEA plates can improve the reliability and reduce the costs of drug safety screenings by

recapitulating drug toxicity mediated through human ion channels on reliable cellular models.

Supplementary data to this article can be found online at <https://doi.org/10.1016/j.taap.2021.115480>.

## Funding

The research leading to these results has received funding from the European Research Council under the European Union’s Horizon 2020 Programme/ERC Grant Agreement no [862078], PoC: MAREP.

## Declaration of Competing Interest

F.D.A and M.D. are inventors of the patent application WO2019116257A1, related to cell optoporation. F.D.A, M.D., F.T., and G.I. are shareholders of the Italian company FORESEE Biosystems srl, which works on cell optoporation systems. G.M. is Chief Executive Officer (CEO) of FORESEE Biosystems srl. N.C. and L.D. declare that there are no conflicts of interest.

## Acknowledgements

The authors thank Dr. Angelo Reggiani and Dr. Rita Scarpelli of the D3 Validation group of IIT for the invaluable discussions.

## References

- 3Brain HD-MEAs, 2021 [WWW Document]. URL. <https://www.3brain.com/products/single-well/hd-mea>.
- 3Brain MultiplEx, 2021 [WWW Document]. URL. [www.3brain.com/biocam-multiplex.html](http://www.3brain.com/biocam-multiplex.html).
- Aiba, T., Shimizu, W., Inagaki, M., Noda, T., Miyoshi, S., Ding, W.-G., Zankov, D.P., Toyoda, F., Matsuura, H., Horie, M., Sunagawa, K., 2005. Cellular and ionic mechanism for drug-induced long QT syndrome and effectiveness of verapamil. *J. Am. Coll. Cardiol.* 45, 300–307. <https://doi.org/10.1016/j.jacc.2004.09.069>.
- Altrocchi, C., de Korte, T., Bernardi, J., Spätjens, R.L.H.M.G., Braam, S.R., Heijman, J., Zaza, A., Volders, P.G.A., 2020. Repolarization instability and arrhythmia by IKr block in single human-induced pluripotent stem cell-derived cardiomyocytes and 2D monolayers. *Eur. Eur. pacing, arrhythmias, Card. Electrophysiol. J. Work. groups Card. pacing, arrhythmias. Card. Cell. Electrophysiol. Eur. Soc. Cardiol.* 22, 1431–1441. <https://doi.org/10.1093/europace/eaab111>.

- Amin, H., Maccione, A., Marinaro, F., Zordan, S., Nieuw, T., Berdondini, L., 2016. Electrical responses and spontaneous activity of human iPSC-derived neuronal networks characterized for 3-month culture with 4096-electrode arrays. *Front. Neurosci.* 10, 121. <https://doi.org/10.3389/fnins.2016.00121>.
- Ando, H., Yoshinaga, T., Yamamoto, W., Asakura, K., Uda, T., Taniguchi, T., Ojima, A., Shinkyo, R., Kikuchi, K., Osada, T., Hayashi, S., Kasai, C., Miyamoto, N., Tashibu, H., Yamazaki, D., Sugiyama, A., Kanda, Y., Sawada, K., Sekino, Y., 2017. A new paradigm for drug-induced torsadogenic risk assessment using human iPSC cell-derived cardiomyocytes. *J. Pharmacol. Toxicol. Methods* 84, 111–127. <https://doi.org/10.1016/j.vascn.2016.12.003>.
- Asahi, Y., Hamada, T., Hattori, A., Matsuura, K., Odaka, M., Nomura, F., Kaneko, T., Abe, Y., Takasuna, K., Sanbusho, A., Yasuda, K., 2018. On-chip spatiotemporal electrophysiological analysis of human stem cell derived cardiomyocytes enables quantitative assessment of proarrhythmia in drug development. *Sci. Rep.* 8, 14536. <https://doi.org/10.1038/s41598-018-32921-1>.
- Asakura, K., Hayashi, S., Ojima, A., Taniguchi, T., Miyamoto, N., Nakamori, C., Nagasawa, C., Kitamura, T., Osada, T., Honda, Y., Kasai, C., Ando, H., Kanda, Y., Sekino, Y., Sawada, K., 2015. Improvement of acquisition and analysis methods in multi-electrode array experiments with iPSC cell-derived cardiomyocytes. *J. Pharmacol. Toxicol. Methods* 75, 17–26. <https://doi.org/10.1016/j.vascn.2015.04.002>.
- Bauman, J.L., Bauernfeind, R.A., Hoff, J. V., Strasberg, B., Swiry, S., Rosen, K.M., 1984. Torsade de pointes due to quinidine: observations in 31 patients. *Am. Heart J.* 107, 425–430. [https://doi.org/10.1016/0002-8703\(84\)90081-4](https://doi.org/10.1016/0002-8703(84)90081-4).
- Berdondini, L., van der Wal, P.D., Guenat, O., de Rooij, N.F., Koudelka-Hep, M., Seitz, P., Kaufmann, R., Metzler, P., Blanc, N., Rohr, S., 2005. High-density electrode array for imaging in vitro electrophysiological activity. *Biosens. Bioelectron.* 21, 167–174. <https://doi.org/10.1016/j.bios.2004.08.011>.
- Berdondini, L., Imfeld, K., Maccione, A., Tedesco, M., Neukom, S., Koudelka-Hep, M., Martinoia, S., 2009. Active pixel sensor array for high spatio-temporal resolution electrophysiological recordings from single cell to large scale neuronal networks. *Lab Chip* 9, 2644–2651. <https://doi.org/10.1039/b907394a>.
- Blinova, K., Stohlman, J., Vicente, J., Chan, D., Johannesen, L., Hortigon-Vinagre, M.P., Zamora, V., Smith, G., Crumb, W.J., Pang, L., Lyn-Cook, B., Ross, J., Brock, M., Chvatal, S., Millard, D., Galeotti, L., Stockbridge, N., Strauss, D.G., 2017. Comprehensive translational assessment of human-induced pluripotent stem cell derived cardiomyocytes for evaluating drug-induced arrhythmias. *Toxicol. Sci.* 155, 234–247. <https://doi.org/10.1093/toxsci/kfw200>.
- Blinova, K., Dang, Q., Millard, D., Smith, G., Pierson, J., Guo, L., Brock, M., Lu, H.R., Kraushaar, U., Zeng, H., Shi, H., Zhang, X., Sawada, K., Osada, T., Kanda, Y., Sekino, Y., Pang, L., Feaster, T.K., Kettenhofen, R., Stockbridge, N., Strauss, D.G., Gintant, G., 2018. International multisite study of human-induced pluripotent stem cell-derived cardiomyocytes for drug proarrhythmic potential assessment. *Cell Rep.* 24, 3582–3592. <https://doi.org/10.1016/j.celrep.2018.08.079>.
- Braam, S.R., Tertoolen, L., van de Stolpe, A., Meyer, T., Passier, R., Mummery, C.L., 2010. Prediction of drug-induced cardiotoxicity using human embryonic stem cell-derived cardiomyocytes. *Stem Cell Res.* 4, 107–116. <https://doi.org/10.1016/j.scr.2009.11.004>.
- Clements, M., Millar, V., Williams, A.S., Kalinka, S., 2015. Bridging functional and structural cardiotoxicity assays using human embryonic stem cell-derived cardiomyocytes for a more comprehensive risk assessment. *Toxicol. Sci.* 148, 241–260. <https://doi.org/10.1093/toxsci/kfv180>.
- Colatsky, T., Fermini, B., Gintant, G., Pierson, J.B., Sager, P., Sekino, Y., Strauss, D.G., Stockbridge, N., 2016. The Comprehensive in Vitro Proarrhythmia Assay (CiPA) initiative - update on progress. *J. Pharmacol. Toxicol. Methods* 81, 15–20. <https://doi.org/10.1016/j.vascn.2016.06.002>.
- Darpó, B., 2001. Spectrum of drugs prolonging QT interval and the incidence of torsades de pointes. *Eur. Hear. J. Suppl.* 3, K70–K80. [https://doi.org/10.1016/S1520-765X\(01\)90009-4](https://doi.org/10.1016/S1520-765X(01)90009-4).
- Dempsey, G.T., Chaudhary, K.W., Atwater, N., Nguyen, C., Brown, B.S., McNeish, J.D., Cohen, A.E., Kralj, J.M., 2016. Cardiotoxicity screening with simultaneous optogenetic pacing, voltage imaging and calcium imaging. *J. Pharmacol. Toxicol. Methods* 81, 15–20. <https://doi.org/10.1016/j.vascn.2016.05.003>.
- Dipalo, M., Melle, G., Lovato, L., Jacassi, A., Santoro, F., Capretti, V., Schirato, A., Alabastri, A., Garoli, D., Bruno, G., Tantussi, F., De Angelis, F., 2018. Plasmonic meta-electrodes allow intracellular recordings at network level on high-density CMOS-multi-electrode arrays. *Nat. Nanotechnol.* 13, 965–971. <https://doi.org/10.1038/s41565-018-0222-z>.
- Food, U.S., Administration, Drug, 1997. FDA proposes to withdraw seldane approval. *FDA Talk Pap.* T97–30 (Jan 13).
- Food, U.S., Administration, Drug, 2000. Janssen Pharmaceutica stops marketing cisapride in the US. *FDA Talk Pap.* T00–6 (Jan 24).
- Garg, P., Garg, V., Shrestha, R., Sanguinetti, M.C., Kamp, T.J., Wu, J.C., 2018. Human induced pluripotent stem cell-derived cardiomyocytes as models for cardiac channelopathies: a primer for non-electrophysiologists. *Circ. Res.* 123, 224–243. <https://doi.org/10.1161/CIRCRESAHA.118.311209>.
- Gintant, G., 2011. An evaluation of hERG current assay performance: translating preclinical safety studies to clinical QT prolongation. *Pharmacol. Ther.* 129, 109–119. <https://doi.org/10.1016/j.pharmthera.2010.08.008>.
- Gintant, G., Sager, P.T., Stockbridge, N., 2016. Evolution of strategies to improve preclinical cardiac safety testing. *Nat. Rev. Drug Discov.* <https://doi.org/10.1038/nrd.2015.34>.
- Guo, L., Abrams, R.M.C., Babiarz, J.E., Cohen, J.D., Kameoka, S., Sanders, M.J., Chiao, E., Kolaja, K.L., 2011. Estimating the risk of drug-induced proarrhythmia using human induced pluripotent stem cell-derived cardiomyocytes. *Toxicol. Sci.* 123, 281–289. <https://doi.org/10.1093/toxsci/kfr158>.
- Harris, K., Aylott, M., Cui, Y., Louttit, J.B., McMahon, N.C., Sridhar, A., 2013. Comparison of electrophysiological data from human-induced pluripotent stem cell-derived cardiomyocytes to functional preclinical safety assays. *Toxicol. Sci.* 134, 412–426. <https://doi.org/10.1093/toxsci/kft113>.
- Hayes, H.B., Nicolini, A.M., Arrowood, C.A., Chvatal, S.A., Wolfson, D.W., Cho, H.C., Sullivan, D.D., Chal, J., Fermini, B., Clements, M., Ross, J.D., Millard, D.C., 2019. Novel method for action potential measurements from intact cardiac monolayers with multiwell microelectrode array technology. *Sci. Rep.* 9, 11893. <https://doi.org/10.1038/s41598-019-48174-5>.
- Huo, J., Kamalakar, A., Yang, X., Word, B., Stockbridge, N., Lyn-Cook, B., Pang, L., 2017. Evaluation of batch variations in induced pluripotent stem cell-derived human cardiomyocytes from 2 major suppliers. *Toxicol. Sci.* 156, 25–38. <https://doi.org/10.1093/toxsci/kfw235>.
- Jackel, D., Bakkum, D.J., Russell, T.L., Muller, J., Radivojevic, M., Frey, U., Franke, F., Hierlemann, A., 2017. Combination of high-density microelectrode array and patch clamp recordings to enable studies of multisynaptic integration. *Sci. Rep.* 7, 978. <https://doi.org/10.1038/s41598-017-00981-4>.
- Jun, J.J., Steinmetz, N.A., Siegle, J.H., Denman, D.J., Bauza, M., Barbarits, B., Lee, A.K., Anastassiou, C.A., Andrei, A., Aydin, C., Barbic, M., Blanche, T.J., Bonin, V., Couto, J., Dutta, B., Gratiy, S.L., Gutnisky, D.A., Hausser, M., Karsh, B., Ledochowitsch, P., Lopez, C.M., Mitelut, C., Musa, S., Okun, M., Pachitariu, M., Putzeys, J., Rich, P.D., Rossant, C., Sun, W.-L., Svoboda, K., Carandini, M., Harris, K.D., Koch, C., O'Keefe, J., Harris, T.D., 2017. Fully integrated silicon probes for high-density recording of neural activity. *Nature* 551, 232–236. <https://doi.org/10.1038/nature24636>.
- Kitaguchi, T., Moriyama, Y., Taniguchi, T., Ojima, A., Ando, H., Uda, T., Otabe, K., Oguchi, M., Shimizu, S., Saito, H., Morita, M., Toratani, A., Asayama, M., Yamamoto, W., Matsumoto, E., Saiji, D., Ohnaka, H., Tanaka, K., Washio, I., Miyamoto, N., 2016. CSAHI study: evaluation of multi-electrode array in combination with human iPSC cell-derived cardiomyocytes to predict drug-induced QT prolongation and arrhythmia—effects of 7 reference compounds at 10 facilities. *J. Pharmacol. Toxicol. Methods* 78, 93–102. <https://doi.org/10.1016/j.vascn.2015.12.002>.
- Kramer, J., Obejero-Paz, C.A., Myatt, G., Kuryshev, Y.A., Bruening-Wright, A., Verducci, J.S., Brown, A.M., 2013. MICE models: superior to the HERG model in predicting torsade de pointes. *Sci. Rep.* 3, 2100. <https://doi.org/10.1038/srep02100>.
- Kussauer, S., David, R., Lemcke, H., 2019. hiPSCs derived cardiac cells for drug and toxicity screening and disease modeling: what micro-electrode-array analyses can tell us. *Cells* 8. <https://doi.org/10.3390/cells8111331>.
- Kuusela, J., Kujala, V.J., Kiviäho, A., Ojala, M., Swan, H., Kontula, K., Aalto-Setälä, K., 2016. Effects of cardioactive drugs on human induced pluripotent stem cell derived long QT syndrome cardiomyocytes. *Springerplus* 5, 234. <https://doi.org/10.1186/s40064-016-1889-y>.
- Liu, Shi, Melchert, Russell B., K, R.H., 1997. Inhibition of L-type Ca<sup>2+</sup> channel current in rat ventricular myocytes by terfenadine. *Circ. Res.* 81, 202–210. <https://doi.org/10.1161/01.RES.81.2.202>.
- Lu, H.R., Vlaminck, E., Hermans, A.N., Rohrbacher, J., Van Ammel, K., Towart, R., Pugsley, M., Gallacher, D.J., 2008. Predicting drug-induced changes in QT interval and arrhythmias: QT-shortening drugs point to gaps in the ICHS7B guidelines. *Br. J. Pharmacol.* <https://doi.org/10.1038/bjp.2008.191>.
- Lu, H.R., Hermans, A.N., Gallacher, D.J., 2012. Does terfenadine-induced ventricular tachycardia/fibrillation directly relate to its QT prolongation and Torsades de pointes? *Br. J. Pharmacol.* 166, 1490–1502. <https://doi.org/10.1111/j.1476-5381.2012.01880.x>.
- Maxwell Biosystems MaxTwo, 2021 [WWW Document]. URL <https://www.mxwbio.com/products/maxtwo-multiwell-microelectrode-array/>.
- Maxwell Biosystems MEAs, 2021 [WWW Document]. URL <https://www.mxwbio.com/products/maxone-mea-system-microelectrode-array/>.
- McNaughton, R., Huet, G., Shakir, S., 2013. An investigation into drug products withdrawn from the EU market between 2002 and 2011 for safety reasons and the evidence used to support the decisionmaking. *BMJ Open* 4, e004221. <https://doi.org/10.1136/bmjopen-2013-004221>.
- Mehta, A., Chung, Y., Sequiera, G.L., Wong, P., Liew, R., Shim, W., 2013. Pharmacoelectrophysiology of viral-free induced pluripotent stem cell-derived human cardiomyocytes. *Toxicol. Sci.* 131, 458–469. <https://doi.org/10.1093/toxsci/kfs309>.
- Mehta, A., Verma, V., Nandihalli, M., Ramachandra, C.J.A., Sequiera, G.L., Sudibyo, Y., Chung, Y., Sun, W., Shim, W., 2014. A systemic evaluation of cardiac differentiation from mRNA reprogrammed human induced pluripotent stem cells. *PLoS One* 9, e103485. <https://doi.org/10.1371/journal.pone.0103485>.
- Melle, G., Bruno, G., Maccafferri, N., Iachetta, G., Colistra, N., Barbaglia, A., Dipalo, M., De Angelis, F., 2020. Intracellular recording of human cardiac action potentials on market-available multi-electrode array platforms. *Front. Bioeng. Biotechnol.* <https://doi.org/10.3389/fbioe.2020.00066>.
- Meyer, T., Boven, K.H., Günther, E., Fejt, M., 2004. Micro-electrode arrays in cardiac safety pharmacology: a novel tool to study QT interval prolongation. *Drug Saf.* <https://doi.org/10.2165/00002018-200427110-00002>.
- Ming, Z., Nordin, C., 1995. Terfenadine blocks time-dependent Ca<sup>2+</sup>, Na<sup>+</sup>, and K<sup>+</sup> channels in Guinea pig ventricular myocytes. *J. Cardiovasc. Pharmacol.* 26, 761–769. <https://doi.org/10.1097/00005344-199511000-00013>.
- Mohammad, S., Zhou, Z., Gong, Q., January, C.T., 1997. Blockage of the HERG human cardiac K<sup>+</sup> channel by the gastrointestinal prokinetic agent cisapride. *Am. J. Phys.* 273, H2534–H2538. <https://doi.org/10.1152/ajpheart.1997.273.H2534>.
- Navarrete, E.G., Liang, P., Lan, F., Sanchez-Freire, V., Simmons, C., Gong, T., Sharma, A., Burrige, P.W., Patlolla, B., Lee, A.S., Wu, H., Beygui, R.E., Wu, S.M., Robbins, R.C.,

- Bers, D.M., Wu, J.C., 2013. Screening drug-induced arrhythmia [corrected] using human induced pluripotent stem cell-derived cardiomyocytes and low-impedance microelectrode arrays. *Circulation* 128, S3–13. <https://doi.org/10.1161/CIRCULATIONAHA.112.000570>.
- Nozaki, Y., Honda, Y., Watanabe, H., Saiki, S., Koyabu, K., Itoh, T., Nagasawa, C., Nakamori, C., Nakayama, C., Iwasaki, H., Suzuki, S., Tanaka, K., Takahashi, E., Miyamoto, K., Morimura, K., Yamanishi, A., Endo, H., Shinozaki, J., Nogawa, H., Shinozawa, T., Saito, F., Kunimatsu, T., 2017. CSAHI study-2: validation of multi-electrode array systems (MEA60/2100) for prediction of drug-induced proarrhythmia using human iPSC-derived cardiomyocytes: assessment of reference compounds and comparison with non-clinical studies and clinical info. *Regul. Toxicol. Pharmacol.* 88, 238–251. <https://doi.org/10.1016/j.yrtph.2017.06.006>.
- Onakpoya, I.J., Heneghan, C.J., Aronson, J.K., 2016. Post-marketing withdrawal of 462 medicinal products because of adverse drug reactions: a systematic review of the world literature. *BMC Med.* 14, 10. <https://doi.org/10.1186/s12916-016-0553-2>.
- Pfeiffer-Kaushik, E.R., Smith, G.L., Cai, B., Dempsey, G.T., Hortigon-Vinagre, M.P., Zamora, V., Feng, S., Ingermanson, R., Zhu, R., Hariharan, V., Nguyen, C., Pierson, J., Gintant, G.A., Tung, L., 2018. Electrophysiological characterization of drug response in hSC-derived cardiomyocytes using voltage-sensitive optical platforms. *J. Pharmacol. Toxicol. Methods.* <https://doi.org/10.1016/j.vascn.2019.106612>.
- Piccini, J.P., Whellan, D.J., Berridge, B.R., Finkle, J.K., Pettit, S.D., Stockbridge, N., Valentin, J.-P., Vargas, H.M., Krucoff, M.W., 2009. Current challenges in the evaluation of cardiac safety during drug development: translational medicine meets the Critical Path Initiative. *Am. Heart J.* 158, 317–326. <https://doi.org/10.1016/j.ahj.2009.06.007>.
- Qu, Z., Xie, L.-H., Olcese, R., Karagueuzian, H.S., Chen, P.-S., Garfinkel, A., Weiss, J.N., 2013. Early afterdepolarizations in cardiac myocytes: beyond reduced repolarization reserve. *Cardiovasc. Res.* 99, 6–15. <https://doi.org/10.1093/cvr/cvt104>.
- Redfern, W.S., Wakefield, I.D., Prior, H., Pollard, C.E., Hammond, T.G., Valentin, J.-P., 2002. Safety pharmacology—a progressive approach. *Fundam. Clin. Pharmacol.* 16, 161–173. <https://doi.org/10.1046/j.1472-8206.2002.00098.x>.
- Sala, L., Bellin, M., Mummery, C.L., 2017. Integrating cardiomyocytes from human pluripotent stem cells in safety pharmacology: has the time come? *Br. J. Pharmacol.* 174, 3749–3765. <https://doi.org/10.1111/bph.13577>.
- Savoji, H., Mohammadi, M.H., Rafatian, N., Toroghi, M.K., Wang, E.Y., Zhao, Y., Korolj, A., Ahadian, S., Radisic, M., 2019. Cardiovascular disease models: a game changing paradigm in drug discovery and screening. *Biomaterials* 198, 3–26. <https://doi.org/10.1016/j.biomaterials.2018.09.036>.
- Scheel, O., Frech, S., Amuzescu, B., Eisfeld, J., Lin, K.-H., Knott, T., 2014. Action potential characterization of human induced pluripotent stem cell-derived cardiomyocytes using automated patch-clamp technology. *Assay Drug Dev. Technol.* 12, 457–469. <https://doi.org/10.1089/adt.2014.601>.
- Viswam, V., Bounik, R., Shadmani, A., Dragas, J., Obien, M., Muller, J., Chen, Y., Hierlemann, A., 2017. High-density mapping of brain slices using a large multi-functional high-density CMOS microelectrode Array system. In: *Int. Solid-State Sensors, Actuators Microsystems Conf. [proceedings]. Int. Conf. Solid-State Sensors, Actuators, Microsystems, 2017*, pp. 135–138. <https://doi.org/10.1109/TRANSDUCERS.2017.7994006>.
- Weiss, J.N., Garfinkel, A., Karagueuzian, H.S., Chen, P.-S., Qu, Z., 2010. Early afterdepolarizations and cardiac arrhythmias. *Heart Rhythm.* <https://doi.org/10.1016/j.hrthm.2010.09.017>.
- Wysowski, D.K., Bacsanyi, J., 1996. Cisapride and fatal arrhythmia. *N. Engl. J. Med.* <https://doi.org/10.1056/NEJM199607253350416>.
- Yonemizu, S., Masuda, K., Kurata, Y., Notsu, T., Higashi, Y., Fukumura, K., Li, P., Ninomiya, H., Miale, J., Tsuneto, M., Shirayoshi, Y., Hisatome, I., 2019. Inhibitory effects of class I antiarrhythmic agents on Na(+) and Ca(2+) currents of human iPSC-derived cardiomyocytes. *Regen. Ther.* 10, 104–111. <https://doi.org/10.1016/j.reth.2018.12.002>.
- Zuppinger, C., Gibbons, G., Dutta-Passecker, P., Segiser, A., Most, H., Suter, T.M., 2017. Characterization of cytoskeleton features and maturation status of cultured human iPSC-derived cardiomyocytes. *Eur. J. Histochem.* 61, 2763. <https://doi.org/10.4081/ejh.2017.2763>.